ELSEVIER

Marine Structures 12 (1999) 131–151

MARINE STRUCTURES

www.elsevier.com/locate/marstruc

Comparative study on mooring line dynamic loading

D.T. Brown[a,*], S. Mavrakos[b]

[a]*Department of Mechanical Engineering, University College, London, Torrington Place, London WC1E 7JE, UK*
[b]*Technical University of Athens, Department of Naval Arch and Marine Engineering, 9 Heroon Polytechniou Ave, GR-157 73 Zografos/Athens, Greece*

Received 1 February 1999; received in revised form 15 March 1999; accepted 6 April 1999

Abstract

This paper presents a comparative study on the dynamic analysis of suspended wire and chain mooring lines. This study was initiated by the International Ship and Offshore Structures Congress (ISSC), Committee I2 (Loads) and is briefly described in the 1997 report presented at Trondheim, Norway. The paper provides more complete documentation of the study. A total of 15 contributions were provided giving analytical results based on time or frequency domain methods for a chain mooring line suspended in shallow water and a wire line in somewhat deeper water. Bi-harmonic top end oscillations representing combined wave and drift induced excitation were specified. The mooring line damping results calculated for chain are compared with limited available experimental data, results provided by the participants showing fair agreement despite the complexity of the numerical methods. Predictions of dynamic tension based on time-domain methods are in broad agreement with each other, the estimates of damping showing more scatter. There are wider discrepancies between results based on frequency-domain methods. © 1999 Elsevier Science Ltd. All rights reserved.

1. Introduction

As hydrocarbon development extends to deeper waters, increasing use is being made of floating production systems with slender member connections between vessel and sea bed. These slender structures principally comprise of risers, tethers, umbilicals and mooring lines.

* Corresponding author. Tel.: 00-44-171-380-7301; fax: 00-44-171-388-0100.
E-mail addresses: d_brown@meng.ucl.ac.uk (D.T. Brown), mavrakos@naval.ntua.gr (S. Mavrakos)

PII: S0951-8339(99)00011-8

Comparative studies investigating flexible risers are well established. In the period between 1988 and 1991, ISSC Committee V7 carried out a comparison of results of two test case configurations from computer programs developed by 11 different institutions for the global dynamic analysis of flexible risers. This study is reported in detail by Larsen [1]. A benchmark study on the cross-sectional structural behaviour of flexibles has also been completed, results being presented by Witz [2]. Here a total of 10 institutions provided numerical data for a Coflexip flexible riser design, results being compared to experimental measurements.

Mooring lines are a key component connecting a floating production vessel to the sea bed. The design of the mooring system, required to hold the vessel within a specified radius above the wellhead, depends on an understanding of the imposed static and dynamic environmental loads. The low-frequency excitation caused by the random waves, and, to a certain extent, wind loading results in resonant motion responses in the horizontal plane leading to high mooring line forces. Previously reported work has shown that the mooring system may under certain circumstances provide up to 80% of the total damping available, thus significantly reducing the vessel resonant excursion and hence peak line tensions. Molin [3] provides an excellent review of the second-order hydrodynamic loading contributions acting on a vessel and moorings, with Brown et al. [4] specifically discussing mooring line damping.

The primary damping components for a moored vessel are induced by current, viscous flow effects, wind, wave drift and the mooring line system. These have been investigated by a number of authors, for example, Triantafyllou et al. [5] gives a good summary. Mooring system damping is caused by line hydrodynamic drag with possible vortex-induced vibration, line internal forces and seabed interaction. Limited work has been performed on the latter which is caused by soil friction leading to reduced tension fluctuations in the grounded portion of line effectively increasing the line stiffness. Thomas et al. [6] indicates that out-of-plane seabed friction and suction effects are negligible in deep water mooring situations whereas in-plane effects can influence the peak tension values.

It is usually considered that the dominating line damping component is caused by hydrodynamic drag, the fluid resistance altering the shape of the line from its undisturbed catenary profile so that, under the action of current loading and more importantly vessel induced excitation, top tensions of higher magnitude than the catenary tension can be induced. The relative movement between line and fluid also induces dissipative forces however that contribute to the total damping imposed on the system. Drag forces for wire lines in particular can be amplified by vortex induced vibrations whereas for chain the amplification is considered negligible [7]. In this context, Triantafyllou et al. [8] have shown that a linear hydrodynamic forcing term is an intrinsic feature of the vortex induced vibrations of long slender cylinders, wire lines being considered as special cases of them, in the lock in regime. They have evaluated this damping coefficient from forced motion tests on rigid cylinders.

Recent work [9] performing experimental tests on large-scale chain sections has shown that drag coefficients associated with combined wave and drift frequency oscillations are significantly higher than those for harmonic flow conditions.

Table 1
Case study participants

Institution	Software	Frequency (FD) or time domain (TD)
Chalmers University of Technology	MODEX	TD
Chalmers University of Technology	MODEX	FD
IFREMER	—	FD
Institut Francais du Petrole	FLEXAN-C	TD
MARIN	DYWFLX95	TD
MARINTEK	R.FLEX	TD
National Technical University of Athens, MIT	CABLEDYN	TD
National Technical University of Athens	NTRANS	FD
Noble Denton Consultancy Services Ltd	DMOOR	TD
Norske Hydro Research Centre	INCL.A-1	FD
Norske Hydro Research Centre	INCL.A-2	FD
Orcina Ltd Consulting Engineers	V.ORCAFLEX	TD
Petrobras SA	ANFLEX	TD
University College London	TDMOOR-DYN	TD
Zentech International	FLEXRISER	TD

In particular, drag coefficients for lines oscillated at wave frequencies in the transverse direction to the drift oscillation direction can be upto 30% higher than those for harmonic oscillation.

Since there is a need for an improved understanding in the hydrodynamic loading and response of mooring lines ISSC Committee I2 initiated a comparative study during the period 1994–1997. The objectives of the study were to report to the ISSC on the current state of the art for dynamic analysis of moorings, and to assess the level of uncertainty in predicting the dynamic tension and mooring induced damping required for global analysis. Quantification of this uncertainty is required for reliability models.

Over 30 organisations were contacted from which 15 contributions were provided for the study. These participants covered the broad spectrum of engineering consultancies, academic institutions and research establishments involved in marine technology. Table 1 gives the list of participants, software names and details as to whether the methods are based on time or frequency-domain formulations.

The rules for participation according to the invitation were that all the participants should perform their analyses and send the results to the authors. These were then collated and sent back for checking. In the distributed tables of results each participant could only identify their own data with responses of the other participants given anonymously. The participants were then left with the choices of accepting their results as final, withdrawing their participation, or revising their response as a result of identifying a source of error. In general, the first pass results were representative of all the models, which is significant considering the considerable number of potential modelling errors.

2. Case study calculation parameters

Two separate sets of calculations were defined. The first set considered a chain mooring in relatively shallow water. This is referred to as System 1. The second set considered a wire mooring in somewhat deeper water and denoted System 2. These conditions generally reflect the usage of the two line types in different water depths. Limited experimental data exist for System 1, see Wichers [10], allowing comparison to be made with calculated values.

Analysis of a single line only was considered. No calculations were performed for wire/chain mixes. These are commonly used in the field but restricting calculations to single lines of wire or chain allows better interpretation and more general applicability of the results.

For each calculation set a base case was defined representing 'typical' conditions. Variations about the base case were then considered. These variations allowed comparison of results for changes in:

Line oscillation amplitude and frequency. This represents wave frequency and wave drift frequency effects causing mooring line oscillation (as a result of vessel top end motion). Only forced sinusoidal oscillation of the line top end about a static offset was considered. It has previously been reported that both the wave-induced oscillation frequency and amplitude have strong influence on damping levels and the combined wave and drift frequency-induced forcing is of specific importance. The contribution of the wave frequency dynamics of the mooring line to the low-frequency damping is thus of particular relevance. In order to investigate this some tests with harmonic forcing only were also specified.

Line orientation. This represents mooring lines at differing azimuth angles relative to the wave drift oscillation direction.

Drag coefficient. Changes in drag (and inertia) coefficient alter the level of line damping. Selection of suitable values depends on line and flow physical characteristics and is made more difficult by the fact that data for many of these characteristics are not available.

The mooring physical properties and site conditions are defined in Table 2 with the line configuration depicted in Fig. 1. Water density of 1025 kg/m^3 was used with the mooring line top end taken at the still water level as shown in Fig. 1. Contributions from the internal (structural) damping of the mooring line were ignored. Likewise, forces induced by in-plane and out-of-plane movement of the line on the seabed were not included.

Where time-domain-based calculations were performed these were run over simulation times corresponding to the larger of the imposed wave or wave drift motion period specified in the following section. Transients were eliminated by allowing a suitable 'start-up' interval.

The definition of drag and added mass coefficients required careful consideration to ensure consistency between results. The definitions of line tangential and normal drag forces (per unit length) used in the study were

$$F_{Dt} = \tfrac{1}{2}\rho C_{Dt} d V|V|, \qquad (1)$$

Table 2
Line physical properties and site conditions

Item	System 1	System 2
Line type	Chain	Wire
Line diameter	140 (mm)	130 (mm)[c]
Total line length (unstretched)	711.3 (m)	4000 (m)
Line weight (in air)	3586.5 (N/m)[b]	800.5 (N/m)[c]
Line weight (in water)	3202.0 (N/m)	664.4 (N/m)[d]
Line axial stiffness EA	1.69×10^9 (N)	1.30×10^9 (N)[e]
Line top tension at equilibrium position[a]	549.9 (kN)	1133.6 (kN)
Top end static horizontal offset - in positive x direction (see Fig. 1)	5.0 (m)	50.0 (m)
Water depth	82.5 (m)	500 (m)
Sea bed inclination	Horizontal	Horizontal
Sea bed friction coefficient	0.0	0.0
Current velocity	See Table 3	0.0 (m/s)

[a]Before applying horizontal static offset.
[b]Vicinay Cadenas S.A., Chain Product Catalogue, CG0-94 (1994).
[c]Bridon Ropes, Steel Wire Ropes and Fittings (1992, p. 103).
[d]API RP 2P, Analysis of Spread Mooring Systems for Floating Drilling Units (1987, p. 15).
[e]DnV, Mobile Offshore Units, POSMOOR (1989).

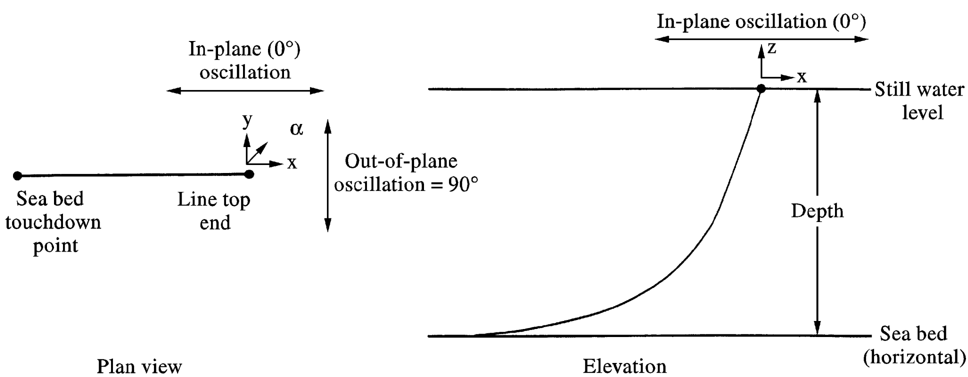

Fig. 1. Mooring line configuration (before static offset or loading applied).

and

$$F_{Dn} = \tfrac{1}{2}\rho C_{Dn} d V|V|, \tag{2}$$

respectively. Line tangential and normal added mass forces (per unit length) were defined as

$$F_{It} = \rho(C_{It} - 1)Aa \tag{3}$$

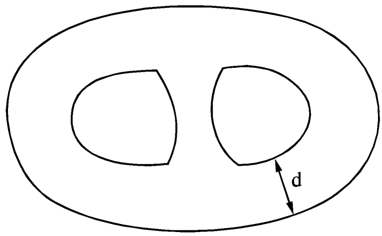

Fig. 2. Definition of chain 'nominal' diameter (d).

and

$$F_{In} = \rho(C_{In} - 1)Aa. \quad (4)$$

In these equations, d represents 'nominal' diameter for chain (see Fig. 2), or wire diameter. The cross-sectional area A for (chain) is based on the nominal diameter, that is ($\pi d^2/4$). Terms V and a represent instantaneous line velocity and acceleration with subscripts t and n denoting, respectively, tangential and normal components.

For each system a base case set of loading conditions was defined and variations from the base case specified. Further detail about the two systems follows:

System 1. Base case (referred to as Test 1.1) loading for System 1 is given in the first line of Table 3.

The specified oscillations were applied after imposing a line top end static offset defined in Table 2. The in-plane oscillation direction is defined as being at 0° to the plane containing the mooring line before loading is applied (see x direction in Fig. 1). The out-of-plane oscillation direction is defined as being at a specified orientation to the in-plane direction.

The following variations from the base case were considered:

- Tests 1.2 – in-plane oscillation corresponding to wave drift frequency motion only.
- Tests 1.3 – in-plane oscillation corresponding to wave frequency horizontal motion only.
- Tests 1.4 – in-plane oscillation corresponding to combined wave horizontal and wave drift frequency motion.
- Tests 1.5 – in-plane oscillation corresponding to wave vertical and wave drift frequency motion, with current; altering the phase relationship ε between wave and drift at time zero.
- Tests 1.6 – out-of-plane oscillation corresponding to wave frequency horizontal and wave drift frequency motion.
- Tests 1.7 – base case with contributor specified hydrodynamic coefficients.

The phase (ε) between wave drift and wave frequency motion (at time $t = 0$) was taken as 0.0° (except for Test 1.5). The phase is defined as

$$\text{motion} = a_d \sin[2\pi(t/T_d) + \varepsilon] + a_w \sin[2\pi(t/T_w)], \quad (5)$$

where a_d and T_d represent drift-induced oscillation amplitude and period, with a_w and T_w being similarly defined for wave oscillations.

System 2. Base case (referred to as Test 2.1) loading for System 2 is given in Table 3. The following variations from the base case were considered:

- Tests 2.2 – in-plane oscillation corresponding to wave drift frequency motion only.
- Tests 2.3 – in-plane oscillation corresponding to wave frequency horizontal motion only.
- Tests 2.4 – in-plane oscillation corresponding to combined wave horizontal and wave drift frequency motion.
- Tests 2.5 – out-of-plane oscillation corresponding to wave frequency horizontal and wave drift frequency motion.
- Tests 2.6 – contributor specified hydrodynamic coefficients.

3. Formulation

The results were reported using numerical and graphical means. In addition tabulated data stored on 3.5 in. floppy disc in ASCII format were provided by some contributors.

The reporting form completed by each contributor also gave limited detail on the background of the numerical models used and the way in which they were run. The time-domain codes generally ramp up the loading over approximately one low-frequency oscillation cycle and use quasi-static analysis/shooting techniques to establish the starting configuration. Spatial discretization of the line is performed using straight bar, elastic truss with lumped masses methods also employed. Quadratic fluid drag loading, added mass, weight and geometric stiffness, etc., are altered at each time step. One innovative method uses the motion response at a characteristic position along the line to estimate fluid loading and hence total tension and damping, whilst retaining essentially a catenary line shape at each time step.

The frequency-domain codes generally linearize quadratic drag making appropriate equivalent energy dissipation assumptions. A novel frequency-domain method uses asymptotic equations to represent an inclined cable under high tension. In the implementation both ends are fixed and the dynamic motion of the line follows the shape of the incremental static deformation with reduced amplitude due to inertia and drag effects.

The data were calculated over an oscillation period, τ, corresponding to that of the wave drift motion. If this was zero then τ was taken as the oscillation period associated with the wave motion.

The following data were reported for each of the tests defined in Table 3.

- Line top tension variation T and its components T_x, T_y and T_z. Maxima and minima were also specified.

Table 3

Test no	Hydrodynamic coefficients				Current[a]	Line top end forced oscillation at						
						Wave drift frequency			Wave frequency			
	C_{Dt}	C_{Dn}	C_{It}	C_{In}	(m/s)	Amp. (m) a_d	Period (s) T_d	Direction	Amp (m) a_w	Period (s) T_w	Direction	Phase (deg) ε
Loading for System 1												
1.1 (Base Case)	0.6	3.2	1.2	2.6	0.0	10.0	100	x	5.4	10.0	x	0.0
1.2.1	0.6	3.2	1.2	2.6	0.0	10.0	100	x	0.0	—	x	0.0
1.2.2	0.6	3.2	1.2	2.6	0.0	20.0	100	x	0.0	—	x	0.0
1.2.3	0.6	3.2	1.2	2.6	0.0	10.0	200	x	0.0	—	x	0.0
1.2.4	0.6	3.2	1.2	2.6	0.0	20.0	200	x	0.0	—	x	0.0
1.3.1	0.6	3.2	1.2	2.6	0.0	0.0	—	x	5.4	10.0	x	0.0
1.4.1	0.6	3.2	1.2	2.6	0.0	10.0	100	x	8.0	10.0	x	0.0
1.4.2	0.6	3.2	1.2	2.6	0.0	10.0	100	x	5.4	13.0	x	0.0
1.5.1	0.6	3.2	1.2	2.6	1.03	20.0	200	x	5.4	10.0	z	0.0
1.5.2	0.6	3.2	1.2	2.6	1.03	20.0	200	x	5.4	10.0	z	270.0
1.6.1	0.6	3.2	1.2	2.6	0.0	10.0	100	α[b]	5.4	10.0	α[b]	0.0
1.6.2	0.6	3.2	1.2	2.6	0.0	10.0	100	y	5.4	10.0	y	0.0
1.7.1	Contributor values				0.0	10.0	100	x	5.4	10.0	x	0.0

Table 3 (*Continued*)

Test no	Hydrodynamic coefficients				Line top end forced oscillation at					
					Wave drift frequency			Wave frequency		
	C_{Dt}	C_{Dn}	C_{It}	C_{In}	Amp. (m)	Period (s)	Direction	Amp. (m)	Period (s)	Direction
Loading for System 2										
2.1 (Base Case)	0.2	1.8	1.2	2.0	30.0	330	x	5.4	10.0	x
2.2.1	0.2	1.8	1.2	2.0	50.0	330	x	0.0	—	x
2.2.2	0.2	1.8	1.2	2.0	30.0	330	x	0.0	—	x
2.3.1	0.2	1.8	1.2	2.0	0.0	—	x	5.4	10.0	x
2.4.1	0.2	1.8	1.2	2.0	30.0	330	x	8.0	10.0	x
2.4.2	0.2	1.8	1.2	2.0	30.0	330	x	5.4	13.0	x
2.5.1	0.2	1.8	1.2	2.0	30.0	330	α[b]	5.4	10.0	α[b]
2.5.2	0.2	1.8	1.2	2.0	30.0	330	y	5.4	10.0	y
2.6.1	Contributor values				30.0	330	x	5.4	10.0	x

[a] Current is in positive x direction – see Fig. 1.
[b] α is defined as 45° to the x direction in the x–y plane – see Fig. 1.

- Line energy dissipation E_x, E_y caused by motion components in the x and/or y direction are given by

$$E_x = \int_o^\tau T_x \frac{dq_x}{dt}\, dt \tag{6}$$

and

$$E_y = \int_o^\tau T_y \frac{dq_y}{dt}\, dt, \tag{7}$$

q_x, q_y being the *sinusoidal* horizontal displacements of the line upper end in the x and y directions associated with the period τ.

Following the first pass return of damping values relatively large differences were noted for the tests with combined wave and drift motions. The reason for this was that a number of contributors erroneously used the displacement q_x calculated using the combined wave and drift frequency displacement. As the damping contribution of interest is that associated with the drift motion the appropriate displacement q_x for use in Eq. (6) is associated with drift frequency oscillation only (if non zero), and is given by

$$q_x = a_d \sin\left[2\pi\left(\frac{t}{T_d}\right) + \varepsilon\right] \tag{8}$$

and similarly for q_y.

Equivalent linearised damping c_x, c_y is given by

$$c_x = \frac{E_x \tau}{2\pi^2 b^2}, \quad c_y = \frac{E_y \tau}{2\pi^2 b^2}, \tag{9}$$

where b is the oscillation amplitude associated with the period τ.

It is noted that linearised damping values (or energy dissipation) are not used directly within time domain mooring analyses to establish vessel motion at drift frequencies and maximum line loads. In practice the contributions from the mooring system caused by line dynamics only influence the vessel response through changes in top end line tension and inclination angle. Furthermore, damping calculations should ideally be performed using irregular waves and responses.

Appropriate linearised damping values are however useful to compare with other system damping sources such as wave drift and viscous contributions for a floating vessel, or internal and seabed damping associated with the mooring. They are also of use when comparing the calculation methods as is being performed here. Simpler frequency-domain models also require estimates of damping.

4. Results

4.1. Maximum tension – contributions

Figs. 3 and 4 show total (catenary plus dynamic) maximum tension over an oscillation cycle for systems 1 and 2, respectively. The term catenary tension refers to

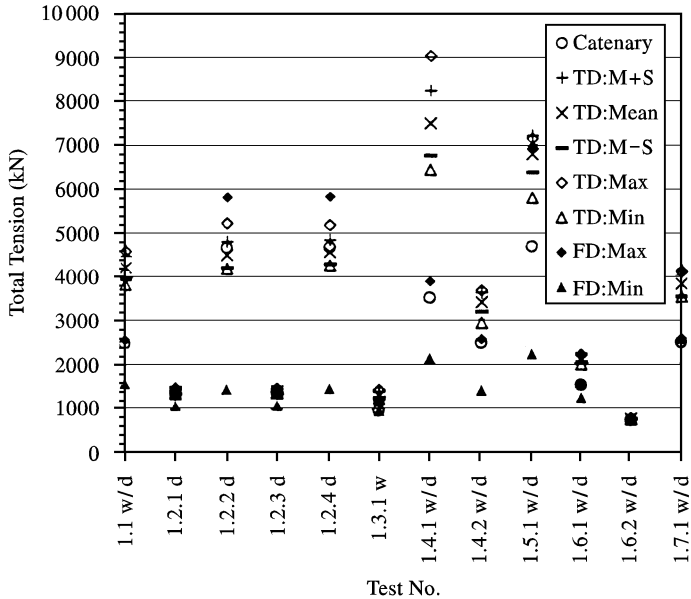

Fig. 3. System 1 – maximum line tension.

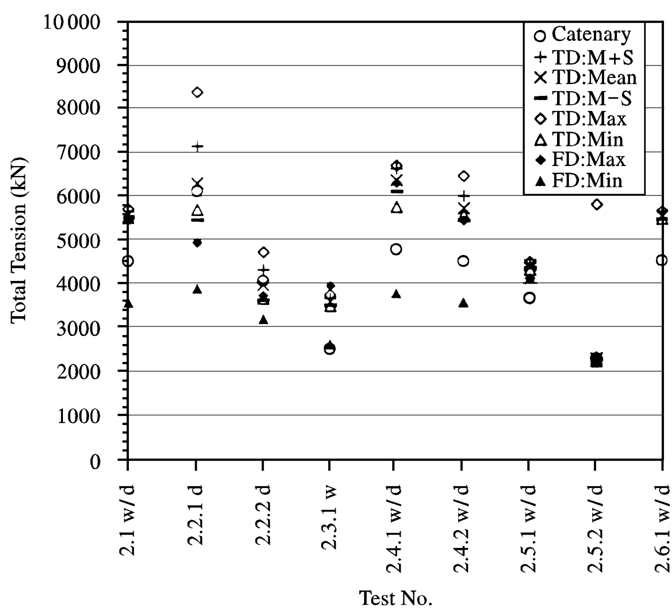

Fig. 4. System 2 – maximum line tension.

the fairlead static tension calculated from the classic catenary equations, associated with the maximum fairlead translation for each test. Consequently no fluid dynamic loading effects are allowed for and the fairlead translation will include contributions from the static horizontal offset, together with the amplitude of motion associated with the imposed drift (*d*), the wave (*w*) or the combined wave/drift (*w*/*d*) motion. Plotted values for the time domain calculations are the mean, mean plus/minus one standard deviation ($M + S$, $M - S$) together with the maximum and the minimum values calculated from the various data provided by contributors. The maximum and the minimum values only are plotted for the frequency-domain calculations. Where the limited contributor data diverge significantly from the majority, results are not used to calculate mean or standard deviation values. Line tensions from catenary theory are also given in the figures. Table 4 also provides mean and standard deviation values from time and frequency-domain calculations together with the catenary tension as defined above.

There is reasonable agreement between predictions of line tension for both systems using time-domain methods. The spread of results are within 20% of the mean value for each of the tests except 2.2.1. Mean values of dynamic tension (i.e. total minus catenary) for drift oscillation only are within 4% of those calculated from catenary theory, whereas there is typically a 20–50% increase with wave or combined wave/drift oscillations. This is discussed further in Section 4.4.

Frequency-domain analyses are generally not in good agreement with time-domain values, particularly for cases where there are high cable motions, because the necessary linearisation breaks down at larger oscillation amplitude.

4.2. Mooring-induced damping – contributions and experiments

Figs. 5 and 6 give calculated line damping values over an oscillation cycle of period τ. Statistical results calculated from the set of contributor data are presented as for the tension amplitude values discussed above.

There is upto 60% variation about the mean for the time-domain linearised damping results as damping calculations depend on the line tension variation throughout the complete oscillation cycle. Frequency-domain damping calculations generally underpredict the time-domain results for the chain line in 82.5 m water depth though they are generally in good agreement with each other. Results for the deep water wire system show wider variation.

System 1 damping values are considered to be in fair agreement with the experimental data for the tests with drift-induced oscillation, showing the same general trends with drift amplitude – see Figs. 7 and 8. Contributor mean values (time domain) are, respectively, +17, +51, −15 and +11% of the measurements for tests 1.2.1–1.2.4. For combined wave and drift (Test 1.5.1) the agreement is not good with contributor mean values overpredicting experiments by 70%.

4.3. Influence of drift-induced top end oscillation

Calculated line damping values are plotted against drift-induced oscillation amplitude for System 1 in Fig. 7 (drift period = 100 s) and 8 (drift period = 200 s).

Table 4

Test number		Total maximum line tension (kN)					Line damping (kNs/m)			
		Time domain		Frequency domain		Catenary	Time domain		Frequency domain	
		Mean (M)	StDev (S)	Mean (M)	StDev (S)		Mean (M)	StDev (S)	Mean (M)	StDev (S)
Total maximum tension and line damping (System 1)										
1.1	*d* – 10 m, 100 s; *w* – 5.4 m, 10 s	4202	258	2070	697	2475	137.6	40.1	110.8	8.2
1.2.1	*d* – 10 m, 100 s	1375	44	1173	174	1374	19.4	2.9	15.6	2.8
1.2.2	*d* – 20 m, 100 s	4497	303	2910	2517	4664	93.6	25.8	31.2	5.6
1.2.3	*d* – 10 m, 200 s	1377	40	1175	172	1374	10.0	6.3	7.8	1.4
1.2.4	*d* – 20 m, 200 s	4556	276	2906	2520	4664	47.9	13.8	15.6	2.8
1.3.1	*w* – 5.4 m, 10 s	1300	70	1079	124	952	87.4	12.0	88.8	16.3
1.4.1	*d* – 10 m, 100 s; *w* – 8.0 m, 10 s	7488	732	3007	1240	3500	171.1	44.4	161.4	16.1
1.4.2	*d* – 10 m, 100 s; *w* – 5.4 m, 13 s	3394	220	1979	825	2475	126.7	37.8	85.6	5.9
1.5.1c	p1 *d* – 20 m, 200 s; *w* – 5.4 m, 10 s	6777	418	4586	3350	4675	264.2	50.6	113.9	5.0
1.5.2c	p2 *d* – 20 m, 200 s; *w* – 5.4 m, 10 s	6746	407	4586	3350	4675	268.2	50.4	113.9	5.0
1.6.1a[a]	45° – 10 m, 100 s; *w* – 5.4, 10 s	2103	78	1358	199	1507	76.6	28.1	58.6	23.7
1.6.1b[a]	45° –10 m, 100 s; *w* – 5.4 m, 10 s	—	—	—	—	—	44.8	18.3	24.1	5.9
1.6.2	90° *d* –10 m, 100 s; *w* – 5.4 m, 10 s	732	10	689	5	695	50.4	20.2	43.0	8.7
1.7.1	*d* – 10 m, 100 s; *w* – 5.4 m, 10 s	3799	288	2562	[b]	2475	122.9	17.5	91.5	[b]
Total maximum tension and line damping (System 2)										
2.1	*d* – 30 m, 330 s; *w* – 5.4 m, 10 s	5586	62	4829	862	4512	910	219	1160	767
2.2.1	*d* – 50 m, 330 s	6288	845	5270	2100	6102	750	85	730	365
2.2.2	*d* – 30 m, 330 s	3941	348	3639	539	4040	446	42	442	218
2.3.1	*w* – 5.4 m, 10 s	3559	79	3435	578	2492	139	33	98	59
2.4.1	*d* – 30 m, 330 s; *w* – 8.0 m, 10 s	6360	261	5398	1115	4771	1087	271	1413	954
2.4.2	*d* – 30 m, 330 s; *w* – 5.4 m, 13 s	5726	278	4832	865	4512	966	167	1155	745
2.5.1a[a]	45° *d* – 30 m, 330 s; *w* – 5.4 m, 10 s	4405	55	4039	105	3647	649	209	897	[b]
2.5.1b[a]	45° *d* – 30 m, 330 s; *w* – 5.4 m, 10 s	—	—	—	—	—	70	27	74	[b]
2.5.2	90° *d* – 30 m, 330 s; *w* – 5.4 m, 10 s	2271	31	2257	28	2270	95	25	94	[b]
2.6.1	*d* – 30 m, 330 s; *w* – 5.4 m, 10 s	5545	88	5332	[b]	4512	875	55	[b]	[b]

[a] Oscillation at 45° to plane of line. Damping values in *x* and *y* direction.
[b] Value not calculated (single or no response).

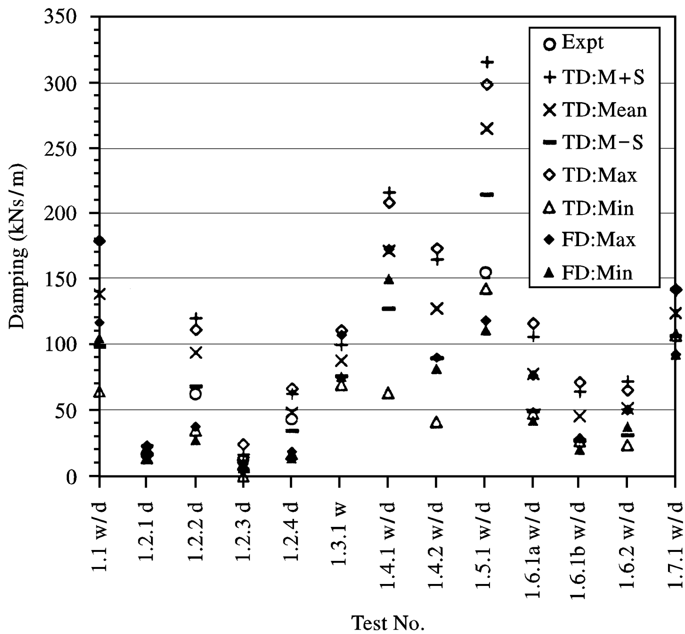

Fig. 5. System 1 – line damping.

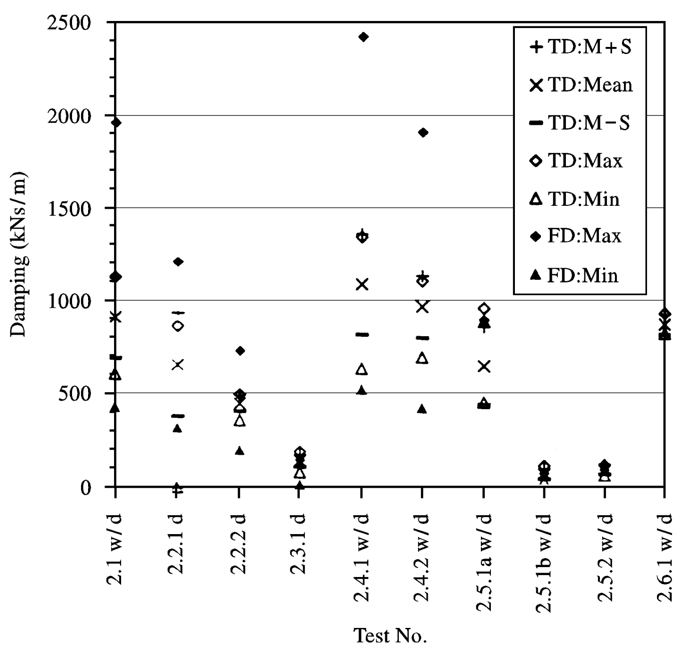

Fig. 6. System 2 – line damping.

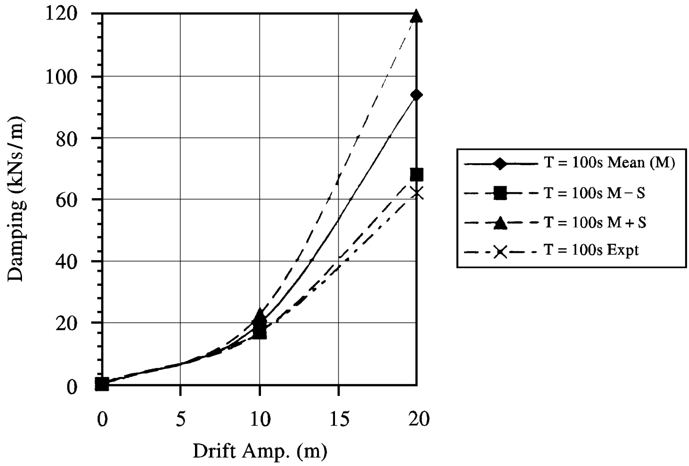

Fig. 7. System 1 line damping vs. drift-induced top end amplitude (drift period = 100 s) – no wave oscillation.

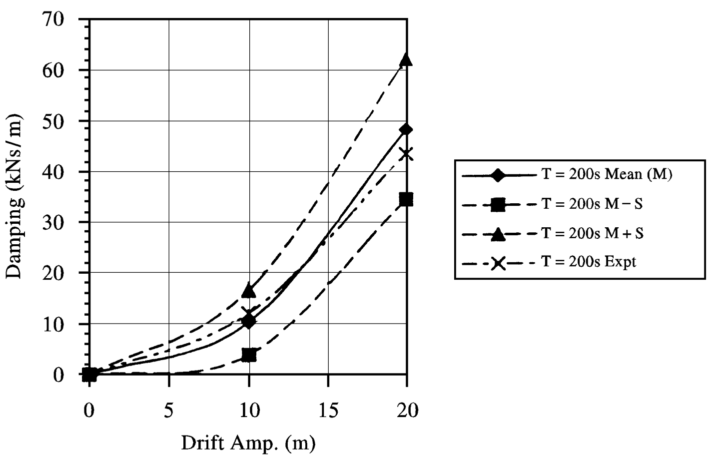

Fig. 8. System 1 line damping vs. drift-induced top end amplitude (drift period = 200 s) – no wave oscillation.

Fig. 9 presents similar data for System 2 (drift period = 330 s). The results are based on time-domain calculations only and are for the tests where no wave oscillations were present. The spread in contributor results is shown in that mean values together with one standard deviation either side of the mean are given. No tension data are provided as maximum dynamic components for these tests were only 3% of the catenary tension.

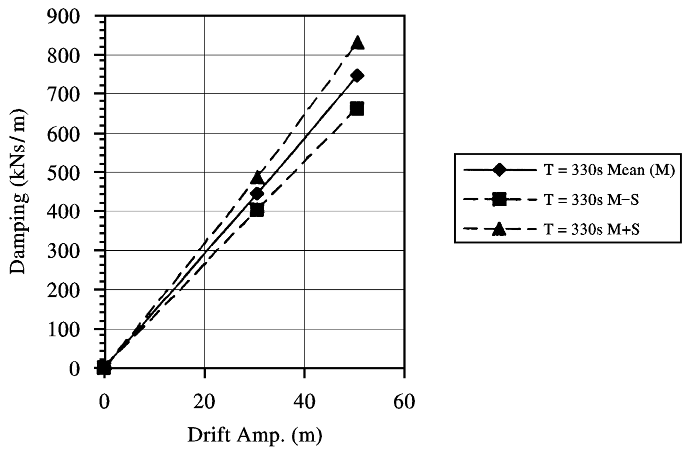

Fig. 9. System 2 line damping vs. drift-induced top end amplitude (drift period = 330 s) – no wave oscillation.

Figs. 7 and 8 indicate that increasing the System 1 drift-induced top end amplitude from 10 to 20 m caused an increase in damping by a factor of approximately 4.5 (based on the mean of contributor data) for both the 100 and 200 s period oscillations. Conversely doubling the oscillation period caused the damping to reduce by 50%. Fig. 9 depicts similar trends with drift-induced amplitude for System 2.

4.4. *Influence of combined drift and wave induced top end oscillation*

Figs. 10 and 11 give dynamic tension components (total tension minus catenary tension) for System 1 (with drift amplitude and period of 10 m and 100 s) and System 2 (with drift amplitude and period of 30 m and 330 s). It is seen that a number of contributions predict total tensions less than the catenary value. A possible reason for this is that the calculation method for catenary tension does not include the stretch of the seabed portion and thus may give slightly conservative tension values. Contributor data may allow stretch of this grounded portion. Figs. 12 and 13 give equivalent line damping data for System 1. The results are based on time domain calculations only and are plotted against wave-induced amplitude with symbols representing wave oscillation periods of 10 and 13 s. There is a consistent trend throughout these results in that both the dynamic tension and the mooring line damping increase significantly in the presence of line wave-induced top end motion. For example Fig. 12 indicates that including top end wave excitation of 5.4 m amplitude at 10 s period for System 1 increases line damping by a factor of 7.1 when compared with the zero wave amplitude situation. This factor becomes 8.8 for 8 m amplitude oscillations. For System 2 the equivalent factors are 2.0 and 2.4. It is difficult to interpret the reasons for the lower System 2 factors due to the several different characteristics of the two systems.

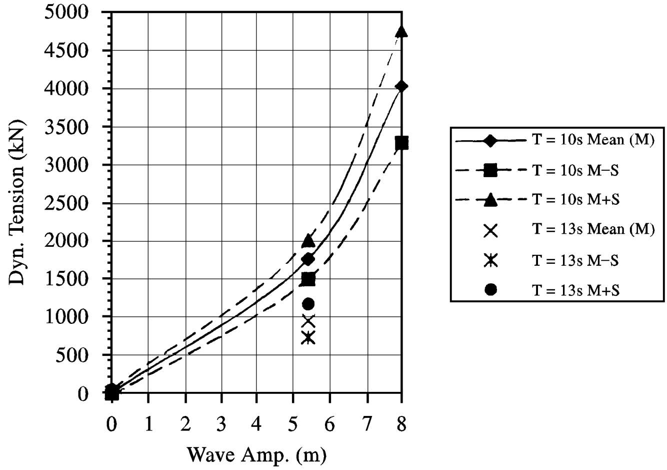

Fig. 10. System 1 maximum dynamic tension vs. wave-induced top end amplitude – with drift oscillation.

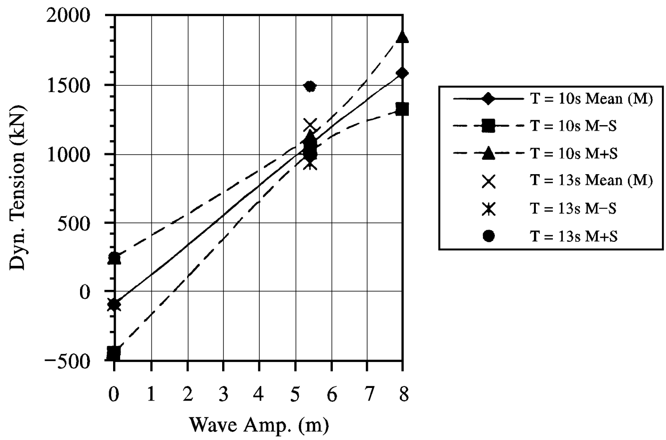

Fig. 11. System 2 maximum dynamic tension vs. wave-induced top end amplitude – with drift oscillation.

4.5. *Influence of phase between wave- and drift-induced top end oscillation*

Tests 1.5.1 and 1.5.2 examined the influence of the phase ε (at time = 0.0) between wave and drift oscillation – see Eq. (5). The results indicated that altering the phase from 0 to 270° made at the most only 4.5% difference to the dynamic tension and 6% difference to the damping. It is noted that for a random wave excitation the phase is considered irrelevant.

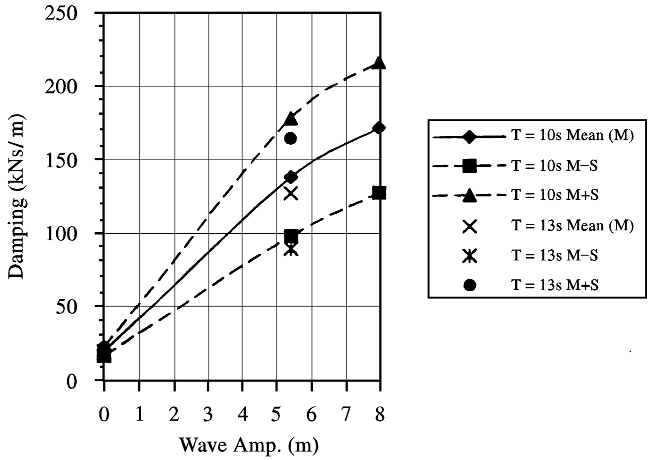

Fig. 12. System 1 line damping vs. wave-induced top end amplitude – with drift oscillation.

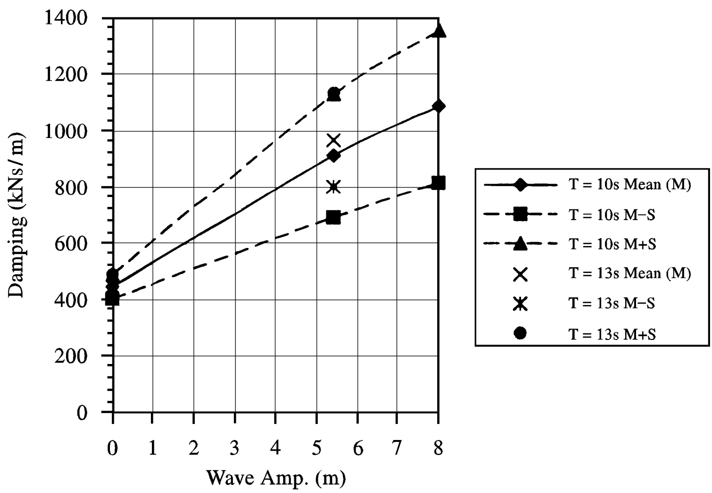

Fig. 13. System 2 line damping vs. wave-induced to end amplitude – with drift oscillation.

4.6. Influence of out-of-plane oscillations

Tests 1.6.1 and 2.5.1 represent oscillations at 45° to the mooring line in the horizontal plane. Damping results for tests 1.6.1a and b together with 2.5.1a and b given in Table 4 relate to appropriate components in the x and y directions (for out-of-plane oscillations at 45°). Tests 1.6.2 and 2.5.2 represent y components for oscillations at 90° to the mooring line in the horizontal plane. These analyses that

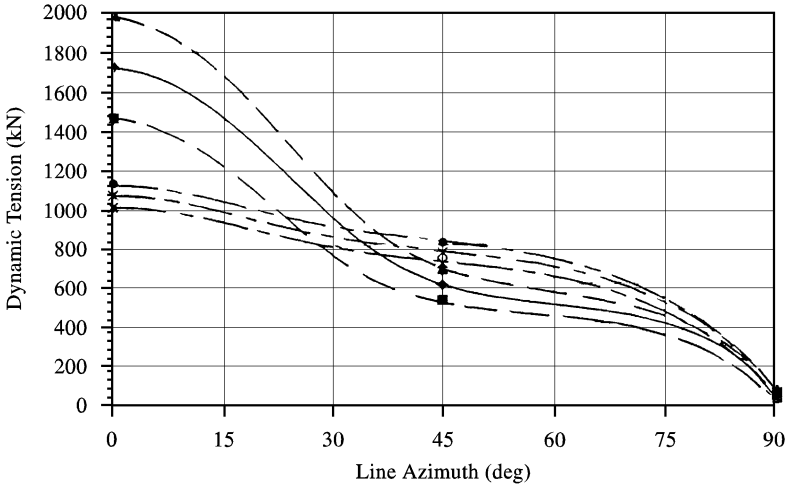

Fig. 14. Systems 1 and 2 maximum dynamic tension vs. line azimuth – combined wave and drift oscillation.

considered out-of-plane oscillation were more prone to misinterpretation by the contributors than the in-line cases.

Results of dynamic tension are plotted against line azimuth angle (relative to oscillation direction) in Fig. 14. In all the cases combined wave and drift oscillations are imposed. The results clearly show that the largest contributions to dynamic tension, and indeed damping, arise when the line oscillations are in the plane of the mooring. It is noted however, that no tests were performed with wave-induced oscillations out of plane with the drift motion as would occur with a floating vessel undergoing surge drift motion together with combined surge and sway wave motion.

4.7. Influence of drag and inertia coefficients

In tests 1.7.1 and 2.6.1 contributors used their own values for hydrodynamic coefficients. Normal drag values for chain and wire in the ranges from 2.2 to 2.5 and 1.0–1.3 were suggested together with normal inertia coefficients of 2.6–4.6 and 2.0–2.6, respectively.

The suggested normal drag values were consistently lower than the values of 3.2 and 1.8 used for the chain and wire tests. In contrast, the contributor suggested normal inertia values were consistently higher than the values of 2.6 and 2.0 used in the pre-defined tests. Three contributors specified tangential drag values for the chain tests in the range from 0.20 to 0.24 somewhat below the pre-specified value of 0.6. Generally values of tangential drag for wire and tangential inertia for both chain and wire were not altered from those pre-specified in the study documentation.

Since a number of the hydrodynamic coefficients were varied simultaneously only limited additional conclusions can be made from the calculations. For System 1 reductions in total tension from 8 to 12%, and damping from 18 to 27% were noted. For

System 2 reductions of upto 7 and 19% for total tension and damping were found. No increase in tension or damping over the base case results were reported.

The advantageous reductions in total tension contrasted by the onerous reductions in mooring-induced damping further emphasise the need to establish consistent values of hydrodynamic coefficients to be used by the design community.

5. Concluding remarks

It is clear from the results of the comparative study that time-domain methods to predict mooring line dynamic tension amplitude are in reasonable agreement with each other. Unfortunately, these methods are usually based on finite-element-type formulations which can be computationally highly intensive, making extensive use in design prohibitively expensive. Further work is required to obtain consistency with more efficient time or frequency domain methods, particularly for situations where large cable motions occur and/or when linearisation assumptions break down. In such cases where non-linear effects, besides the ones originating from the quadratic drag, have to be taken into account, time domain solutions appear at present to offer the only possibility for giving reliable results.

Predictions of damping which depend on the tension variation and line angle over an oscillation cycle show a wider range of scatter. The damping levels contribute to the reduction in floating vessel resonant drift motion and so are of key importance.

The numerical methods require input values of hydrodynamic drag and inertia coefficient. The study has highlighted a range of coefficient values used by the design community for identical mooring systems of simple make up. It is clear that further work such as that performed by Brown et al. [9] is required in the selection of these coefficients, and in particular hydrodynamic drag, leading to more consistent design practice.

Both frequency- and time-domain calculations need further validation against experimental measurements. The experiments in restricted water depth require appropriate scaling of both cable elastic stiffness and its free-falling velocity, as shown by Papazoglou et al. [11]. This leads in many cases to unrealistic full-scale designs due to improper scaling of the line's static configuration through the imposed limited water depth. Full scale measurements, or at least experiments as performed by Mavrakos et al. [12] in appropriately selected deep water to ensure both static and dynamic similitude between full scale and the scaled down configuration, would provide the most accurate information. Additional work is required, however, to conduct full scale measurements and importantly to make their results openly available.

Hybrid methods that allow non-linear loading and that utilise time-domain methods should be further investigated to assess their applicability limits. Certainly they can be computationally efficient as the exact line profile need not necessarily be established on a continuous basis. They should however be used with care in situations where the bottom line interaction effects need to be accurately taken into account, thus requiring the instantaneously suspended cable's length. In such cases, fully numerical schemes that allow the integration of the cable's dynamic equations in space and time and take into account the bending effects seem to provide the most reliable solution.

A shortcoming of the present study is that it was limited to harmonic or bi-harmonic excitation of a single chain or wire line. It would be beneficial for a future study to consider more realistic loading conditions, line layouts and component mixes including fibre moorings and attached submerged buoys along the lines.

Acknowledgements

On behalf of ISSC Committee I2-Loads, the authors wish to express their gratitude to all the contributors for their involvement. The authors also wish to thank the research staff in the Department of Mechanical Engineering at University College London for their help in collating the results.

References

[1] Larsen CM. Flexible riser analysis – comparison of results from computer programs. Marine Struct 1992;5:103–19.
[2] Witz JA. A case study in the cross-section analysis of flexible risers. Marine Struct 1996;9:885–904.
[3] Molin B. Second order hydrodynamics applied to a moored structure – a state of the art survey Schiffstechnik 1994;4:59–84.
[4] Brown DT, Lyons GJ, Lin HM. Advances in mooring line damping. J Soc Underwater Tech 1995;21:5–12.
[5] Triantafyllou MS, Yue DKP, Tein DYS. Damping of moored floating structures. Proceedings of the OTC, Houston, USA, Paper 7489, 1994. pp. 215–24.
[6] Thomas DO, Hearn GE. Deep water mooring line dynamics with emphasis on seabed interaction effects. Proceedings of the OTC, Paper 7488, 1994. pp. 203–14.
[7] NTNF, FPS 2000 Research Programme – Mooring Line Damping, Part 1.5, E. Huse. Marintek Rpt, 1991.
[8] Triantafyllou MS, Gopalkrishnan R, Grosenbaugh MA. Vortex induced vibrations in a sheared flow: a new predictive method. In: Faltinsen O et al., editors. Proceedings of the International Conference on Hydroelasticity in Marine Technology. Trondheim, Norway: Balkema, Rotterdam, 1994, pp. 31–7.
[9] Brown DT, Lyons GJ, Lin HM, Large scale testing for mooring line hydrodynamic damping contributions at combined wave and drift frequencies. in: Proc. BOSS, vol. 2. Oxford: Pergamon, 1997, pp. 397–406.
[10] Wichers JEW, Huijsmans RHM. Contribution of hydrodynamic damping induced by mooring chains on low frequency motions. Procedings of the OTC, Paper 6218, 1990, pp. 171–81.
[11] Papazoglou VJ, Mavrakos SA, Triantafyllou MS. Non linear cable response and model testing in water. J Sound Vibr 1990;140(1):103–15.
[12] Mavrakos SA, Papazoglou VJ, Triantafyllou MS, Chatjigeorgiou J. Deep water mooring dynamics. Marine Struct 1996;9:181–209.